Self-Assembly Behavior of Amphiphilic Poly(amidoamine) Dendrimers with a Shell of Aniline Pentamer

ARTICLE *in* LANGMUIR · SEPTEMBER 2013

Impact Factor: 4.46 · DOI: 10.1021/la403063t · Source: PubMed

Langmuir

Article

pubs.acs.org/Langmuir

Self-Assembly Behavior of Amphiphilic Poly(amidoamine) Dendrimers with a Shell of Aniline Pentamer

Wei-I Hung,[†,‡] Chi-Hao Chang,[†] Ya-Han Chang,[†] Pei-Shan Wu,[†] Chih-Bing Hung,[†] Kung-Chin Chang,[†] Mei-Chun Lai,[†] Sheng-Chieh Hsu,[†] Yen Wei,[§] Xin-Ru Jia,*[,∥] and Jui-Ming Yeh*[,†,¶]

[†]Department of Chemistry, Center for Nanotechnology at CYCU, Chung-Yuan Christian University, Chung Li 32023, Taiwan, R. O. C.

[‡]Institute of Chemistry, Academia Sinica, 128, Section 2, Academia Road, Taipei 115, Taiwan 11529, R. O. C.

[§]Department of Chemistry, Tsinghua University, Beijing 100084, China

[∥]Department of Polymer Science and Engineering, College of Chemistry and Molecular Engineering, Peking University, Beijing 100871, China

[¶]Institute of Biomedical Technology of Chung-Yuan Christian University

Supporting Information

ABSTRACT: A series of amphiphilic poly(amidoamine) dendrimers (PAMAM, G2−G5) composed of a hydrophilic core and a hydrophobic shell of aniline pentamer (AP) were synthesized and characterized. The modified dendrimers self-assembled to vesicular aggregates in water with the critical aggregation concentration (CAC) decreased in the order of G2 > G3 > G4 > G5. It was found that the modified dendrimers self-organized into spherical aggregates with a bilayer vesicular structures and that the dendrimers in higher generation have more order structure, which may be attributed to the crystallization induced by the compacted effect of AP segments. In addition, larger spherical vesicles were observed under acidic and alkaline conditions, as compared with sizes of aggregates in neutral medium. At low pH, the tertiary amine groups of PAMAM-AP were transformed to ammonium salts; the polarons were formed from AP units by doping with strong acids, thereby leading to the stability of vesicular aggregates being better than that in double distilled water. Nevertheless, in high pH environment, the deprotonation of PAMAM-AP caused the enhancement of $\pi-\pi$ interactions, resulting in generation of twins or multilayered vesicles.

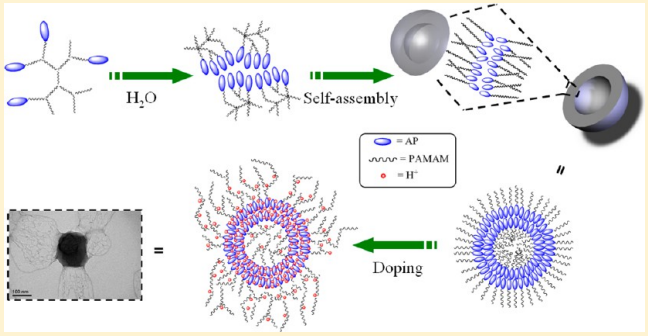

INTRODUCTION

Over the past decade, dendritic polymers have attracted much attention with the emergence of a large variety of synthetic approaches, fundamental studies on the structure, properties of these sui generis materials, and their potential applications.[1−3] Dendrimers are monodisperse molecules with well-defined and perfectly branched architectures. Modification and functionalization of the dendritic periphery are useful methods of forming supramolecular assemblies from the dendritic molecules.[4−7] Numerous intermolecular forces affect the self-assembly behavior of amphiphilic molecules, including the ion−ion, ion−dipole, dipole−dipole, hydrogen bonding, cation−π, $\pi-\pi$, van der Waals forces, and CH_2-CH_2.[4] When compared to linear amphiphiles, dendritic amphiphiles with highly branched structures can not only exhibit more stable micellar aggregates but also yield unimolecular micelles as well. As examples, Newkome et al.[8] reported the first divergent synthesis of amphiphilic dendrimers by functionalizing the nonpolar core of their arboral dendrimers with a polyol periphery that rendered these macromolecules stable in water. Fréchet and co-workers[9] successfully utilized the first asymmetric dendrimer (amphiphilic segmented dendrimer) containing ether end groups in one hemisphere and methyl esters in the other to illustrate micellar properties. Meijer and co-workers[10] evaluated the self-assembly behavior of amphiphilic dendrimers based on poly(propyleneimine) (PPI) dendrimers modified with long hydrophobic chains at five different generations. Their study unvailed that the soft hydrophobic chains at the periphery can form aggregates; however, the rigid hydrophobic shell around the dendritic core could not be dispersed in solution. Jia and co-workers[11−13] were the first to demonstrate that the formation of ordered aggregates from poly(amidoamine) (PAMAM) dendrimers modified with different short hydrophobic rigid chromophores. These results show that the unusual molecular architecture of dendritic polymers provides a suitable framework to achieve unique photophysical and

Received: March 26, 2013
Revised: September 1, 2013
Published: September 6, 2013

photochemical properties when the aggregation behavior happened. Nevertheless, these aggregates could be observed barely at the lower generations ranging from PAMAM G0 to G3 since the driving force of short hydrophobic rigid shell is not powerful enough to perform the self-assembly phenomena at high generations. Gröhn et al.[14] reported that the vesicles only with PAMAM G8 can successfully self-assemble by modifying electrostatic counterions. Moreover, the tailorable structure of amphiphilic dendrimers have led to their exploration for a range of applications, including scaffolds for drug[15,16] and gene[17] delivery. In addition, a few studies[10,18] have discussed the stability of amphiphilic dendrimers in different pH environments. According to our past work,[19] we found that the electron transition of the $\pi_B-\pi_Q$ band red-shifted and the size of PAMAM-AP G2 decreased in an alkaline medium. This suggests, in the diverse pH environments, the self-assembly behavior of amphiphilic PAMAM-AP will be influenced exponentially. Herein, we synthesized PAMAM dendrimers (PAMAM G2−5), using the aniline pentamer (AP) as a shell. Distinct from the previous studies,[11−13] these dendrimers in higher generations (G = 4 and 5) still can self-assemble into bilayer vesicles owing to the $\pi-\pi$ interactions of the long aromatic segments—the aniline pentamer (AP). To the best of our knowledge, this is the first report to demonstrate a series of different generation PAMAM based dendrimers with AP groups; they exhibit a very low CAC and are stable in water for over one month. Furthermore, since both of PAMAM and AP are the pH-sensitive species, the variation in the size of these spherical aggregates with pH was also evaluated. These bilayer structures were characterized and explored, based on TEM, SEM, AFM, DLS, and XRD.

EXPERIMENTAL SECTION

Materials. PAMAM dendrimers (G = 2, 3, 4, and 5) were synthesized and further purified according to literature methods.[20,21] The emeraldine base form of the aniline pentamer (AP) and AP modified with carboxyl-protected amino groups (AP-COOH) have also been reported in the literature.[19,21−23] *N*,*N*′-Dicyclohexylcarbodiimide (99%, Fluka), ethylenediamine (99%, J.T. Baker), methyl acrylate (MA, 99%), and succinic anhydride (SA, 97%) were obtained from Alfa Aesar. 4-(Dimethylamino)pyridine (DMAP, 99%) was purchased from Sigma-Aldrich. 1-Methyl-2-pyrrolidinone (NMP) was dried by removing water as benzene azeotrope. Dimethyl sulfoxide (DMSO) and *N*,*N*-dimethylformamide (DMF) were dried over CaH_2 and then distilled under reduced pressure prior to use. Other reagents were commercially available and used as received.

Synthesis of Amphiphilic PAMAM Dendrimers G2−5 Containing AP Shell (PAMAM-AP G2−5). Synthesis of PAMAM-AP G5. Amphiphilic PAMAM-AP G2−5 dendrimers were synthesized via a previously reported route.[19] In brief, PAMAM G5 (0.353 g, 0.0123 mmol) dissolved in a DMF/NMP solution was mixed with AP-COOH (0.87 g, 1.57 mmol), DCC (1.3 g, 6.3 mmol), and DMAP (0.19 g, 1.57 mmol) in the same solvent. After 5 days of vigorous stirring at −5 °C, the suspension was filtered to remove dicyclohexylurea (DCU) formed and repeatedly washed with 0.25 M HCl until the filtrate became clear. The solid was collected and then dissolved in DMSO and dialyzed in dialysis membranes (with M_w cutoff of 2000) to remove AP-COOH. After the removal of AP-COOH, the condensation product was precipitated by decanting into aqueous HCl solution. The HCl-doped PAMAM-AP G5 was then dedoped to its base form by treatment with 250 mL of aqueous NH_4OH solution (pH = 9) at room temperature for 4 h. The product was collected by filtration and was washed with a large amount of H_2O. A pale blue powder was obtained after drying the residue under reduced pressure in a vacuum oven at 40 °C for 24 h. Yield: 30%. ^{1}H NMR (DMSO-d_6, ppm): δ 7.15−6.66 (528 H, aromatic ring of AP), δ 1.72−0.97 (2022 H, $-CH_2-$ of PAMAM G5). ^{1}H NMR, COSY ^{1}H/^{1}H spectra for PAMAM-AP G2−5 are provided in the Supporting Information. In order to quantify the extent of the reaction of AP with the amino group ($-NH_2$) on the dendrimer periphery, the AP calibration curve (R^2 = 0.9977) was constructed by employing UV−vis spectroscopy based on the 313 nm $\pi-\pi^*$ transition of the aromatic benzene ring and the 600 nm transition from the phenyl to the quinoid, in addition to utilizing NMR and MS data. An average of 25 AP units were found on the PAMAM G5 surface based on NMR analysis, whereas the calibration curve determined from UV−vis spectroscopy indicated an average of 26 AP units on the exterior surface of PAMAM G5. The reactivity between PAMAM G5 and AP is 19.5%, which is lower than that of the PAMAM-AP G2−4 congeners,[19] and the corresponding data are summarized in Table 1.

Table 1. Relationships of PAMAM-AP G2−5 with the Average Number of AP per PAMAM, the Degree of AP Substitution, Weight Ratio, and CAC in Water

	PAMAM-AP			
	G2	G3	G4	G5
AP[a]	5	7	13	25
degree of substitution (%)	31.3	21.9	20.3	19.5
weight ratio[b] (%)	24.4	28.6	29.7	31.2
CAC (M)	5.7×10^{-6}	2.9×10^{-6}	1.6×10^{-6}	7.3×10^{-7}

[a]The average number of AP per PAMAM. [b]The weight ratio of AP/PAMAM-AP based on the TGA diagram.

Process for Producing Self-Assembled Vesicles. In a typical process,[24] 4.26 mg of finely powdered PAMAM-AP G5 was dissolved in DMSO. The resulting solution was placed in a dialysis bag (M_w cutoff of 2000 for PAMAM-AP G2−5) and dialyzed against doubly distilled water five times within 48 h to remove the DMSO; the outer dialysis solution was replaced for each dialysis run. The solution was then centrifugal to remove impurities. The self-assembled vesicles with a concentration of 10^{-5} M were thus obtained.

Measurement. *Microscopy.* Transmission electron microscopy (TEM) measurements were performed on a JEOL JEM-1400 TEM (Tokyo, Japan) instrument operated at an accelerating voltage of 120 kV. The size and distribution of the bilayer vesicle particles were determined by placing a drop of sample solution (concentration: 10^{-5} M) on carbon-coated copper grids, removing the excess of water by blotting with a filter paper, drying the grid under ambient atmosphere for 1 h, and negative staining by addition of a drop of 2 wt % uranyl acetate solution. Atomic force microscopy (AFM) observations were conducted on a psia AFM (XE-100) using a sample preparation technique that is similar to that used for TEM analysis, but using a new sheet glass as the substrate. Scanning electron microscopy (SEM) samples were prepared by drop-casting 1−2 drops of the diluted samples onto a piece of silicon wafer. SEM images were acquired with a JEOL JSM-7600F field emission scanning electron microscope.

Other Characterization Techniques. ^{1}H NMR and ^{13}C NMR spectra were recorded on Bruker Advance 300 and 400 MHz spectrometers at room temperature using $CDCl_3$, D_2O, and d_6-dimethyl sulfoxide as solvents. UV−vis spectra were obtained at room temperature using a UV−vis double-beam spectrophotometer (JASCO V-630/Lenses) in order to determine the critical aggregation concentration (CAC). Powder X-ray diffraction patterns of the samples were acquired on a PANalytical X-ray powder diffractometer (X'Pert Pro (MRD) PW 3040/60) operating at 45 kV and 40 mA employing Cu Kα radiation (λ = 0.154 nm) with a time per step of 31.75. The size distribution of the vesicles was further confirmed at room temperature using various pH adjusted aqueous media, based on the principles of dynamic laser light scattering (DLS), by utilizing a Brookhaven 90Plus Particles Size Analyzer (Brookhaven Instruments Corporation, Holtsville, NY).

Scheme 1. Schematic Illustration of Structure of PAMAM-AP G2−5 (n = the Average Number of AP Groups)

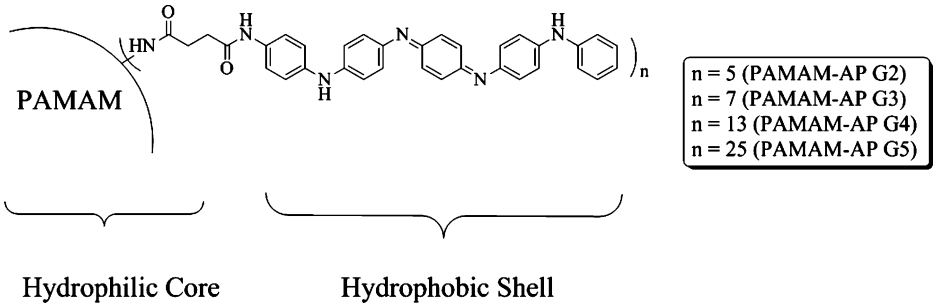

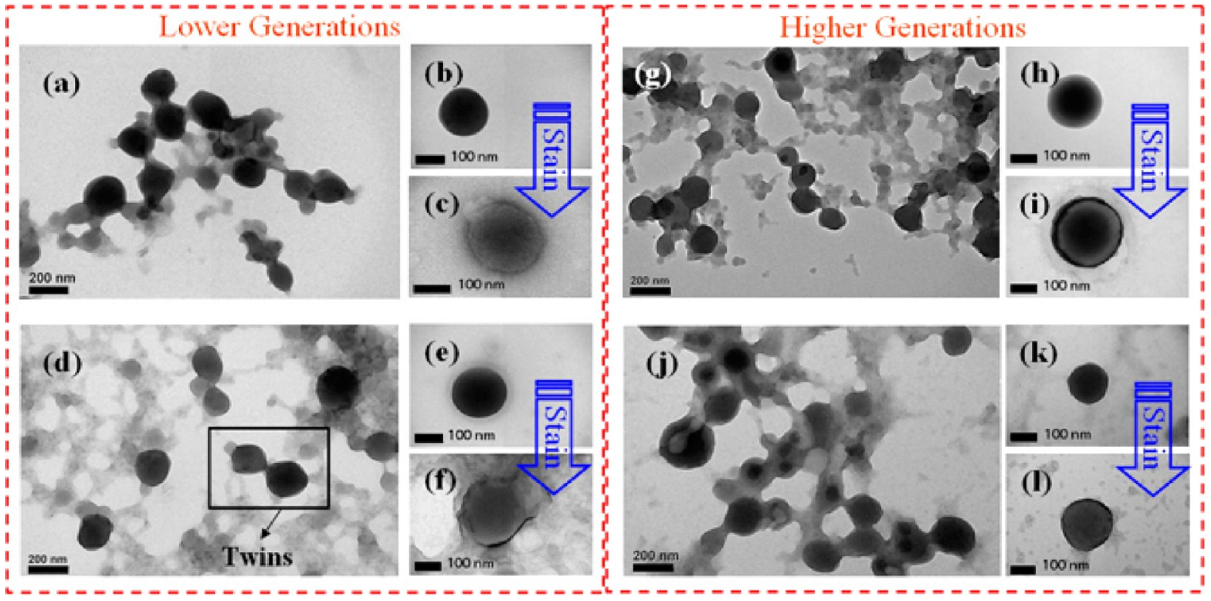

Figure 1. TEM images of lower-generation PAMAM-AP G2 (a, b), PAMAM-AP G3 (d, e), and higher-generation PAMAM-AP G4 (g, h) and PAMAM-AP G5 (j, k) with and without negative staining using uranyl acetate. Corresponding TEM images (c, f, i, and l). Concentration: 10^{-5} M.

RESULTS AND DISCUSSION

Self-Assembly of PAMAM Dendrimers G2−5 Having an AP Shell (PAMAM-AP G2−5). The amino groups at the end of the AP units were converted to the carboxyl species via reaction with succinic anhydride; this group was then connected to the periphery of the PAMAM dendrimers via the standard DCC coupling method. The peripherally AP-modified PAMAM dendrimers having the hydrophobic shell and hydrophilic aminoamine interior were expected to display amphiphilic properties, as shown in Scheme 1. These architectures also readily undergo self-organization to generate spherical aggregates with bilayer vesicular structures due to the strongly hydrophobic nature of the emeraldine APs in the dendrimers. The aggregation and self-assembly behavior of the amphiphilic dendrimers, PAMAM-AP G2−5, are presented below.

Morphology and Aggregation Behavior. PAMAM-AP G2−5 dendrimers can be considered as amphiphilic molecules based on the coexistence of the long hydrophobic rigid AP unit at the periphery and the hydrophilic interior branches in the same molecule. The aggregation behavior of these dendrimers in water was investigated by means of transmission electron microscopy (TEM), atomic force microscopy (AFM), and scanning electron microscopy (SEM). Solvents play a crucial role in the self-assembly process; the solvent affinity of regions of these amphiphilic dendrimers may vary, with selective solvent for a particular block. Thus, a block that is miscible with the solvent is exposed on the outer surface of the aggregates, whereas the immiscible block is located inside of the aggregates. However, prediction of the resulting self-assembled morphologies from a designed amphiphile structure becomes complicated if the packing of the hydrophobic chains is crystalline.[25] Israelachivili proposed an optimal surface area per polar headgroup, which depends on the packing parameter, $P_c = v/(a_0 l_c)$.[26] If $1/2 \leq P_c \leq 1$, bilayers with a spontaneous curvature (vesicles) are produced (vide infra). Moreover, the morphology of the self-assemblies depends on a number of structural factors and experimental conditions such as the hydrophobic and hydrophilic chain lengths and ratios, their distribution, the stereochemistry of the polymer chain, concentration, and so forth. The formation of bilayer vesicles, generally, can be attributed to the amphiphilic structure of dendrimers possessing aliphatic chains and aromatic systems.[11−13,27] The TEM images of PAMAM-AP G2−5 shown in Figure 1 demonstrate the formation of spherical aggregates, all between 100 and 200 nm in diameter. As the dendrimer generation increased from G2 to G5, the size of the bilayer vesicles gradually decreased. The particle size distribution of the PAMAM-AP G2−5 species were determined using dynamic laser light scattering (DLS) and are discussed in the ensuing section. The bilayer structure of the vesicles was also clearly confirmed from TEM images with and without negative

dx.doi.org/10.1021/la403063t | Langmuir 2013, 29, 12075−12083

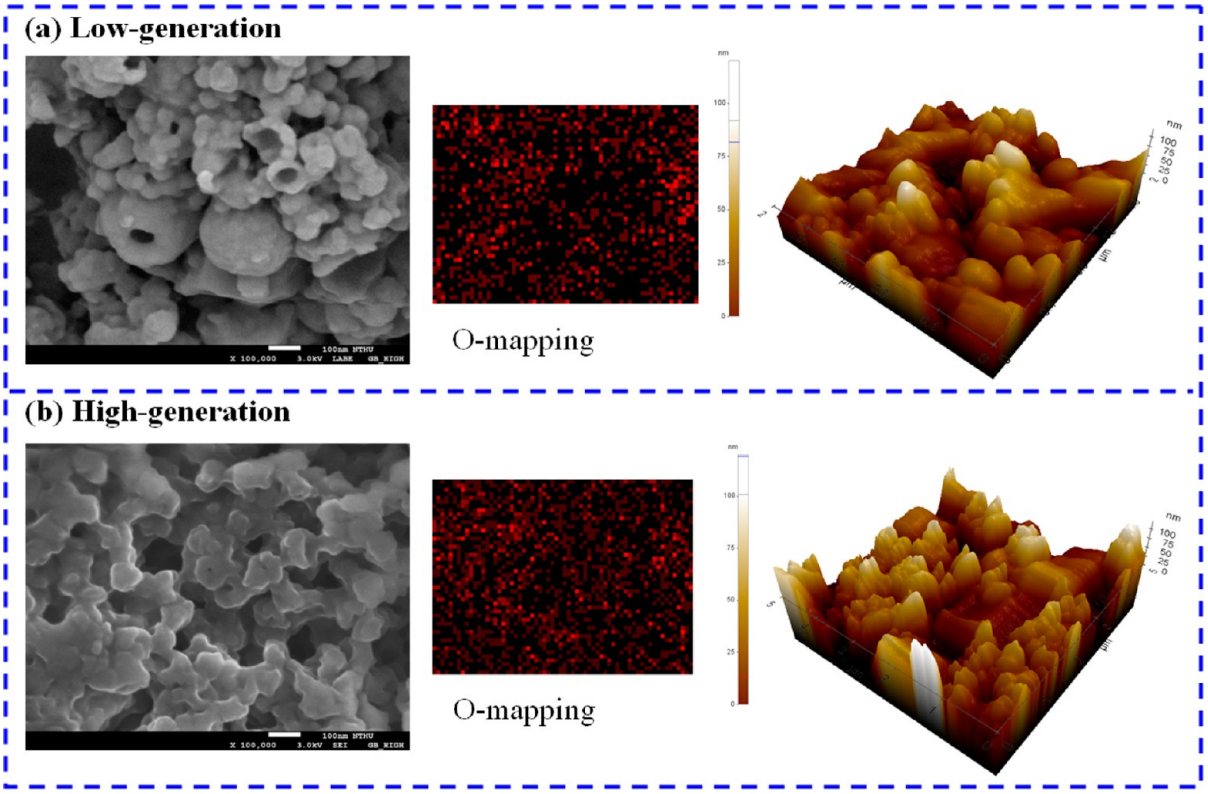

Figure 2. SEM images, O-mapping, and AFM images of (a) low-generation PAMAM-AP G2 and (b) high-generation PAMAM-AP G4.

staining. The hydrophobic interphase of the bilayer appears black due to the high electron density of the APs before staining as shown in Figure 1a,d,g,j. Because the flexible hydrophilic dendritic branches are located in the outer layer indicated as gray, these vesicles are very adhesive. Self-adhesion via H-bonding interaction of the branches occurs more readily for the higher-generation dendrimers than the lower-generation counterparts. Furthermore, as the generation increased from G2 to G5, the size of the bilayer vesicles gradually decreased (Figure 1b,e,h,k) owing to the loose structures of the lower-generation dendrimers and the reduced number of AP chains in increasing generations succeeding PAMAM-AP G2.[19] Moreover, the average thickness of the hydrophobic interphase was about 1.7−2.1 nm (determined from TEM images without negative staining), which is smaller than the head-to-head distances of the AP double layer (theoretical value = 4.8 nm). This discrepancy might be due to the strongly $\pi-\pi$ interactions of the long hydrophobic rigid AP units in the self-assembled architectures. In addition, the mass of the shell of AP was calculated quite accurately via TGA curve[28−30] with summarizing data in Table 1. After electron staining with uranyl acetate, exactly reversed images were observed as shown in Figure 1c,f,i,l. The outer and inner layers of the vesicles appear in black with negative staining, indicating that the hydrophilic dendritic branches are localized in this region. The vesicle particles observed after staining with uranyl acetate were apparently larger than the original one. In addition, multiple aggregates containing two vesicles (twins) and multivesicles were observed as shown in Figure 1a,d,g,j. The higher-generation PAMAM-AP G5 sample was characterized by a large number of multiple aggregates due to the increased number of hydrophobic AP segments in the periphery group of the PAMAM dendrimers. This observation has been found to confirm the self-assembly progress of PAMAM-AP G2 and G5. The self-assembled vesicles of PAMAM-AP G5 shows more fine and stable structure than PAMAM-AP G2 in aqueous solution. Furthermore, fusion and fission structures were also observed (see Figure S-9), the formation mechanism of which is consistent with our previous report.[13] Interestingly, for the higher-generation, G4 and G5 species, the PAMAM dendrimers peripherally modified with strongly hydrophobic APs formed ordered aggregates in water. As shown in Figure 2, SEM and AFM images of PAMAM-AP G2 and G4 revealed the formation of vesicles of various diameter based on self-assembly. Very dilute aqueous solutions (10^{-6}−10^{-7} M) of the higher- (G4) and lower-generation (G2) dendrimers were dropped onto the sheet glass. It should be noted that the diameter of the vesicular structures was increased to a lesser extent for the lower-generation PAMAM dendrimers, i.e., PAMAM-AP G2. Moreover, the outer layers of the vesicles, i.e., the hydrophilic dendritic branches, were evaluated via EDX O-mapping images, also presented in Figure 2. From the above data, the detailed aggregate characteristics of dendrimers furnished by the packing parameters are listed in Table S-1. The P_c values for PAMAM-AP G2−5 were found to be in the range of 0.5−1.0, indicating that the aggregates possess bilayer vesicular structures. The theoretical prediction corresponds to the exact observation from TEM.

Critical Aggregation Concentration. The self-assembly behavior, triggering by hydrophobic interactions among long linear aromatic rings, the peripheral groups of dendrimers, has not been reported thus far. Herein, the aggregates could be observed even in higher-generation dendrimers, i.e., PAMAM-AP G4 and G5, which might be due to the strongly hydrophobic nature of AP and $\pi-\pi$ interactions between species of compatible polarity, resulting in mutual attraction. In

dx.doi.org/10.1021/la403063t | *Langmuir* 2013, 29, 12075−12083

order to gain insight into the aggregation behavior, the critical aggregation concentration (CAC) of these dendrimer aggregates was quantified by monitoring the intensity change of the 331 nm $\pi-\pi^*$ transition of the aromatic benzene ring and the 600 nm transition from the phenyl to the quinoid. Figure 3

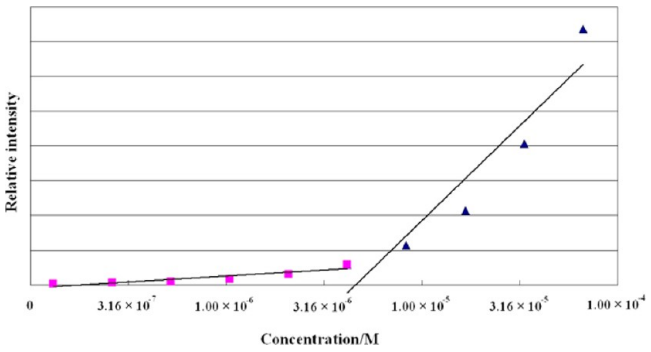

Figure 3. Relationship between $\pi_B-\pi^*_B$ transition and concentration of PAMAM-AP G2. The break point indicates the critical aggregation concentration (CAC).

shows the UV−vis spectral changes of the 331 nm $\pi-\pi^*$ transition of the aromatic benzene ring with increasing concentration of PAMAM-AP G2. Table 1 summarizes the relationship between the dendrimer generation (G2−G5) and the CAC values. The CAC values decrease gradually on moving from G2 to G5, suggesting that formation of these aggregates is favored in the order G5 > G4 > G3 > G2. The CAC values are generally very low ($10^{-6}-10^{-7}$ M) as expected for these amphiphilic dendrimers.[13] Unlike most studies, the higher-generation (G4 and G5) amphiphilic PAMAM-AP dendrimers possess a stronger driving force for the self-organization in term of the $\pi-\pi$ interactions of AP and H-bonding interactions between the dendrimer branches. Therefore, within the range of G2−5, the dendrimers in higher generations tend to aggregate because of the increase in AP units and H-bonding interaction among the dendrimer branches. To the best of our knowledge, this is the first observation of the formation of bilayer vesicles by higher generations of poly(amidoamine) dendrimers functionalized with AP.

Evaluation of Stability of Vesicular Aggregates. To gain insight into the stability of the amphiphilic molecular architecture under different pH environment, absorption spectroscopy was used to detect the upper layer solution of the PAMAM-AP G2 and G5 vesicular aggregates at a concentration of 10^{-5} M. The solutions were stored in the dark at room temperature, and their molar extinction coefficients were measured once every 2 days. Figure 4a shows the long-term temporal evolution of the UV−vis spectra of PAMAM-AP G5 in doubly distilled water. The peaks at 330 nm (corresponding to the $\pi-\pi^*$ transition of the aromatic benzene ring) and at 636 nm (i.e., the transition from phenyl to quinoid) gradually decreased in intensity with time. Notably, the intensity of the characteristic peak at ca. 330 nm was significantly decreased after 28 days. A comparison of the stability of PAMAM-AP G2 and PAMAM-AP G5 at various pH is also presented in the Figure 4b. It should be noted that the PAMAM-AP G5 and G2 can exhibit more stable under acidic conditions (pH = 3.0) than under neutral (pH = 7.0) and alkaline conditions (pH = 9.0). Moreover, the molar extinction coefficient of PAMAM-AP G5 shows little change over one month. Figure 4b also shows a decreased of absorptivity to approximately 37.7% (G2) and 10.4% (G5) after 35 days under acidic conditions (pH = 3.0) and 87.7% (G2) and 11.2% (G5) after 21 days (pH = 7.0) and 40.2% (G2) and 23.5% (G5) after 14 days under alkaline conditions (pH = 9.0). This provides good evidence of the better long-term stability of the higher-generation amphiphilic PAMAM-AP G5 species relative to lower generation. In addition, it was found that PAMAM-AP G5 exhibited more stable in an acidic medium. This might be because PAMAM-AP G5 possesses more hydrophilic dendritic branches in the outer layer and a lower CAC value. The temporal stability of the amphiphilic dendrimer self-assemblies and their biological application is currently under way. To develop a better understanding of the self-assembly behavior of PAMAM-AP G2−5, the variation of pH on self-assembly was measured by using transmission electron microscopy (TEM) and the dynamic laser light scattering (DLS) technique.

Effect of Variation of pH on Self-Assembly. The effect of pH variation on the lower (G2) and higher (G4) generations of amphiphilic dendrimers was evaluated based on the postulate that the size of PAMAM-AP should change during doping (pH = 3.0) and dedoping (pH = 9.0), mainly due to the conversion of the tertiary amines in PAMAM into ammonium salts[31−33] or polaron production in the AP segments.[19] As shown in Figure

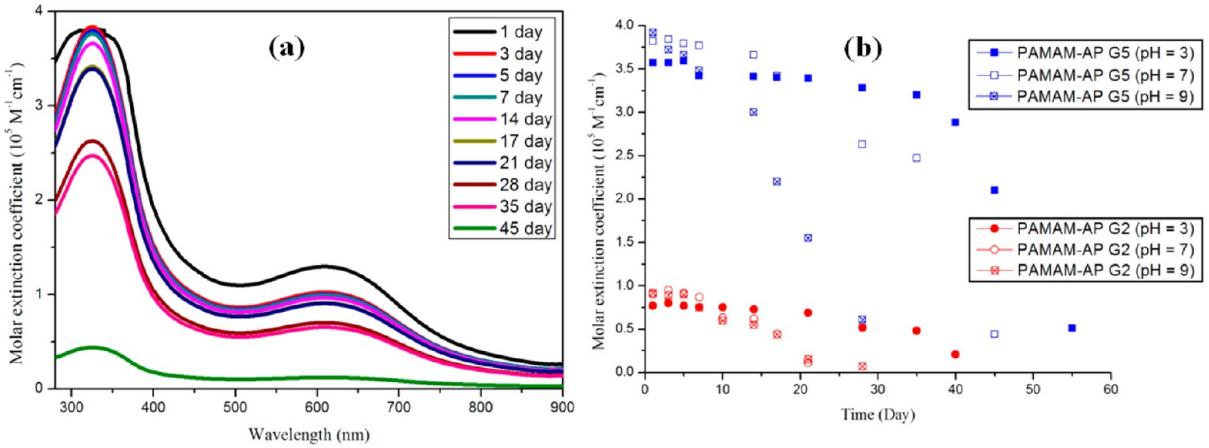

Figure 4. (a) Temporal stability of self-assemblies of PAMAM-AP G5 in doubly distilled water. (b) Absorptivity PAMAM-AP G2 and G5 with time based on the 330 nm absorption at various pH.

dx.doi.org/10.1021/la403063t | Langmuir 2013, 29, 12075−12083

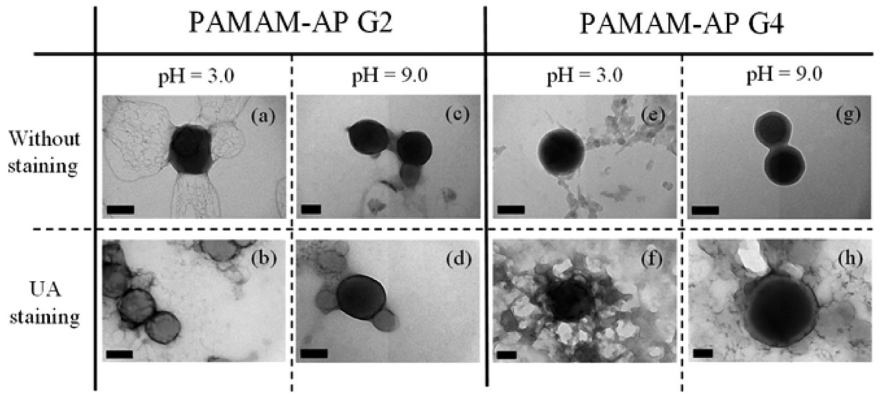

Figure 5. TEM images of the lower- (G2) and higher-generation (G4) aggregates without (a, c, e, g) and with (b, d, f, h) negative staining at various pH values (scale bar: 100 nm).

Scheme 2. Schematic Illustration of Vesicle Generation for (a) PAMAM-AP G2−5 in Water and (b) under Acidic Conditions (pH = 3.0)

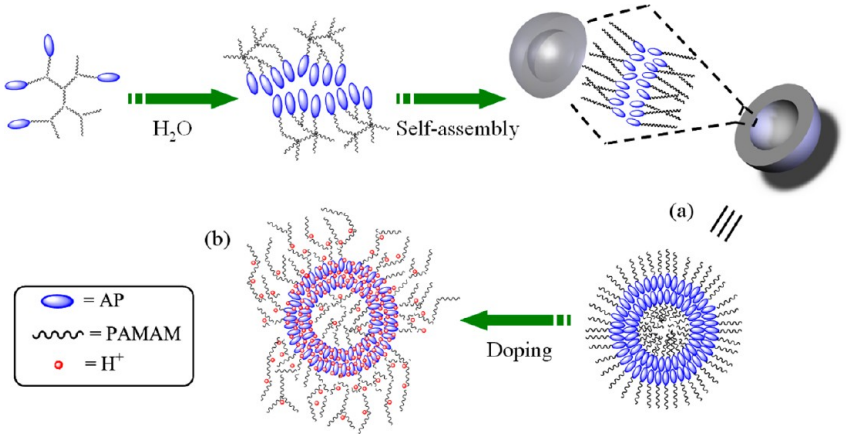

5a, the increased charge on PAMAM-AP G2 at low pH resulted in the hydrophilic dendritic branches located in the outer layer becoming extended. This may indicate the conversion of the tertiary amines into ammonium salts to form ion pairs in PAMAM. Therefore, low pH leads to a "dense shell" and nonuniform void spacings.[34] Moreover, it can be seen that spherical aggregates (or bilayer vesicles) are formed from three or more individual amphiphilic dendrimers, and protonation of the tertiary amines results in electrostatic swelling. In comparison, Figure 5c shows that the PAMAM-AP G2 assembly become more compact under alkaline conditions, which is attributed to the $\pi-\pi$ interactions of the strongly emeraldine APs. The larger number of twins observed at high pH formed by the "dense core" owing to the fully deprotonated (uncharged) dendrimer,[34] and these aggregate more readily by H-bonding interactions than at low pH. Negative staining was performed using PAMAM-AP G2 under acidic (Figure 5b) and alkaline (Figure 5d) conditions, respectively. High-generation PAMAM-AP G4 aggregates at different pH values and their corresponding electron staining images display the same vesicular structure, as shown in Figure 5e−h. Owing to the spherical aggregates formed under alkaline conditions, the bilayer thickness of the vesicles increased slightly on moving from lower to higher generation. The formation of bilayer vesicles of PAMAM-AP G2−5 was facilitated by the flexible hydrophilic dendritic branches and strongly hydrophobic emeraldine AP. As previously reported,[11,13] AP units may possess a stronger reverse force than phenyl, naphthyl, pyrenyl, and dansyl chromophores. The hydrophilic branches of the dendrimers extend out to occupy more room in water. To minimize the energy in water, the long hydrophobic aromatic moieties of the dendrimers shrink and pack together in parallel with the aid of $\pi-\pi$ interactions to form the hydrophobic interphase between the bilayers as illustrated in Scheme 2a. Changing the pH from neutral to acidic caused the hydrophilic dendritic branches in the outer layer to be converted from tertiary amines into ammonium salts with concomitant doping of emeraldine AP. The size change induced by the acidic effect led to an increase in the thickness of the outer layer and the hydrophobic layer, as shown in Scheme 2b. Furthermore, a decrease in the curvature of the hydrophobic layer and an increase of the aggregate size (twins or multivesicles) were observed under alkaline conditions using DLS.

Effect of pH on Particle Size Distribution. DLS evaluation (intensity as the analysis approach) of the self-assembly of lower- (G2 and G3) and higher-generation (G4 and G5) amphiphilic dendrimers was used to determine the effect of pH on the size of the aggregates of the amphiphilic dendrimers as shown in Figure 6. Under neutral conditions, the size of these vesicles decreases as the dendrimer generation increases from G2 to G5. This result might be interpreted in term of the favored self-assembly process of higher generations due to an increase in the number of strongly hydrophobic APs, leading to increased $\pi-\pi$ interactions. As expected, it was found

dx.doi.org/10.1021/la403063t | *Langmuir* 2013, 29, 12075−12083

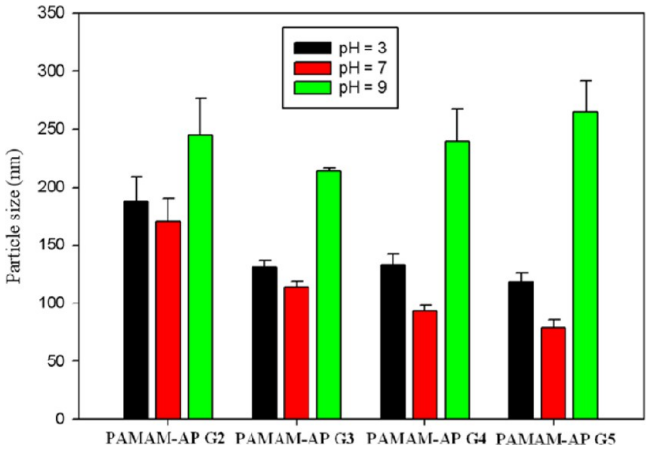

Figure 6. Particle size distribution of PAMAM-AP G2−5 at various pH.

that as the pH value decreased, the size of the vesicles of PAMAM-AP on the hydrophilic dendritic branches became more loosely packed with volume expansion. This may be attributed to the conversion of the tertiary amines into ammonium salts in PAMAM and the emeraldine base AP becoming the emeraldine salt AP during acid doping. However, at high pH, PAMAM-AP is deprotonated, resulting in increased $\pi-\pi$ interactions and the packing of AP chains becoming more ordered and more facile aggregation via H-bonding interactions. Therefore, alkaline conditions minimize the energy required for aggregation of these vesicles.

Self-Assembly Driving Force Analysis. X-ray diffraction (XRD) analyses of the samples were used to elucidate the possible molecular packing patterns of PAMAM-AP G2−5. Figure 7a shows a broad peak in the XRD profile of PAMAM

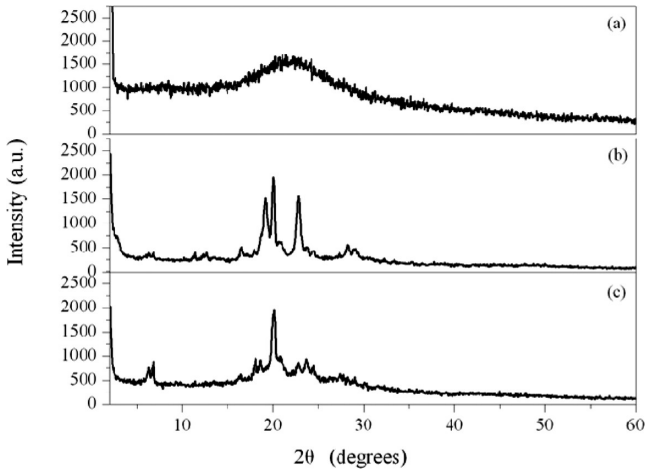

Figure 7. WAXD patterns of (a) PAMAM G2, (b) AP, and (c) AP-COOH.

G2, characteristic of diffraction by an amorphous polymer. AP is a kind of rigid molecular assembly with three main intense peaks, two of which are centered at about 19° (d = 4.6 nm) and 20° (d = 4.4 nm), ascribed primarily to the periodicity parallel to the oligomer chain, and the other at 23° (d = 3.9 nm), corresponding to the periodicity perpendicular to the transverse direction (Figure 7b).[35,36] Furthermore, AP appended with carboxyl-protected amino groups (AP-COOH) by reaction with succinic anhydride has a molecular, length of about 30 Å, which is larger than the length of 25 Å for AP. A significant decrease in 2θ value at 23° for the diffraction plane of transverse direction is observed on moving from AP to AP-COOH, as shown in Figure 7c. The WAXD patterns for the PAMAM-AP G2−5 assembly are also shown in Figure 8. Based

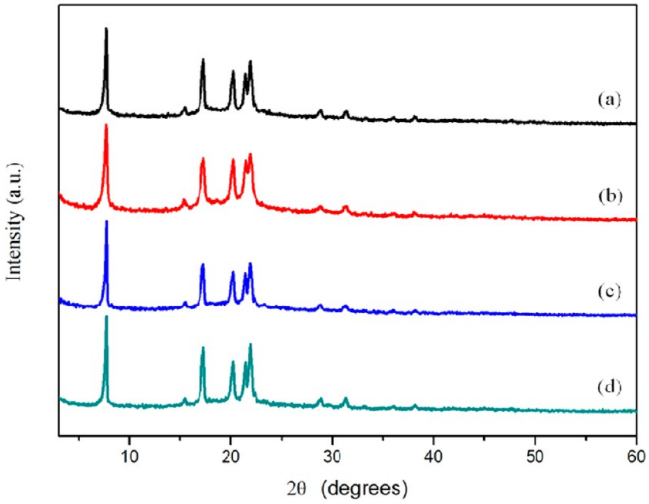

Figure 8. WAXD patterns of (a) PAMAM-AP G2, (b) PAMAM-AP G3, (c) PAMAM-AP G4, and (d) PAMAM-AP G5.

on our previous report,[19] owing to the AP chains being attached to the PAMAM core, the arrangement of the AP chains becomes more order. The WAXD patterns presented in Figure 8a−c show several new peaks (compared to AP-COOH, (Figure 7c) at about 7.7° (d = 11.5 nm), 15.5° (d = 5.7 nm), 17.2° (d = 5.2 nm), 28.9° (d = 3.1 nm), and 31.4° (d = 2.8 nm). These results support the conclusion that the amphiphilic dendrimers can undergo self-assembly and became more order of the structure. Moreover, the intensity of the primary diffraction peaks of PAMAM-AP at 2θ = 15.5°, 17.2°, and 20.2° increased as the generation was increased from G2 to G5. For PAMAM-AP, the intensity of these peaks was essentially affected by increase in the generation of amphiphilic dendrimer, illustrating the increased order due to enhanced $\pi-\pi$ interactions of the strongly emeraldine APs.

CONCLUSION

PAMAM dendrimers possessing the strongly hydrophobic nature of emeraldine AP as the shell can self-assebly, even at higher generation (G5), into spherical aggregates with bilayer vesicular strucutures in different media, based on TEM images after negative staining. Amphiphilic dendrimers form more ordered assemblies as the generation augmented owing to the introduction of the crystalline structure of the APs onto the PAMAM dendrimer. Furthermore, as the dendrimer generation increased from G2 to G5, the size and CAC gradually diminished, for the stronger driving force of PAMAM-AP induced by the $\pi-\pi$ interactions of the long and rigid emeraldine AP units. In addition, the higher generation of PAMAM-AP, the more promising stability they bear. Moreover, the PAMAM-AP G2−5 have miscellaneous conformations in various pH milieux: low pH leads to a "dense shell" and nonuniform void spacing; nevertheless, in high pH environment, the deprotonation results in "dense core". In our ongoing study, these PAMAM-AP, after all, will potentially serve as

dx.doi.org/10.1021/la403063t | Langmuir 2013, 29, 12075−12083

avant-garde dendritic carriers for gene and drug delivery, for their desirable self-assembly performances.[37−39]

■ ASSOCIATED CONTENT

Supporting Information

Additional details. This material is available free of charge via the Internet at http://pubs.acs.org.

■ AUTHOR INFORMATION

Corresponding Authors

*E-mail juiming@cycu.edu.tw (J.-M.Y.).
*E-mail xrjia@pku.edu.cn (X.-R.J.).

Notes

The authors declare no competing financial interest.

■ ACKNOWLEDGMENTS

Financial support of this research by Ministry of Education, Taiwan, R. O. C., Mainland Affairs Council, NSC 101-2632-M-033-001-MY2, and department of Chemistry, Center for Nanotechnology at CYCU, is gratefully acknowledged.

■ REFERENCES

(1) Jansen, J. F. G. A.; de Brabander-van den Berg, E. M. M.; Meijer, E. W. Encapsulation of guest molecules into a dendritic box. *Science* **1994**, *266*, 1226−1229.

(2) Frechet, J. M. Functional polymers and dendrimers: reactivity, molecular architecture, and interfacial energy. *Science* **1994**, *263*, 1710−1715.

(3) Tomalia, D. A.; Naylor, A. M.; Goddard, W. A. Starburst dendrimers: Molecular-level control of size, shape, surface chemistry, topology, and flexibility from atoms to macroscopic matter. *Angew. Chem., Int. Ed.* **1990**, *29*, 138−175.

(4) Rosen, B. M.; Wilson, C. J.; Wilson, D. A.; Peterca, M.; Imam, M. R.; Percec, V. Dendron-mediated self-assembly, disassembly, and self-organization of complex systems. *Chem. Rev.* **2009**, *109*, 6275−6540.

(5) Grayson, S. M.; Fréchet, J. M. J. Convergent dendrons and dendrimers: from synthesis to applications. *Chem. Rev.* **2001**, *101*, 3819−3867.

(6) Shimizu, T.; Masuda, M.; Minamikawa, H. Supramolecular nanotube architectures based on amphiphilic molecules. *Chem. Rev.* **2005**, *105*, 1401−1443.

(7) Astruc, D.; Boisselier, E.; Ornelas, C. Dendrimers designed for functions: from physical, photophysical, and supramolecular properties to applications in sensing, catalysis, molecular electronics, photonics, and nanomedicine. *Chem. Rev.* **2010**, *110*, 1857−1957.

(8) Newkome, G. R.; Yao, Z.; Baker, G. R.; Gupta, V. K. Cascade molecules: A new approach to micelles. *J. Org. Chem.* **1985**, *50*, 2003−2004.

(9) Hawker, C. J.; Wooley, K. L.; Fréchet, J. M. J. Unimolecular micelles and globular amphiphiles: dendritic macromolecules as novel recyclable solubilization agents. *J. Chem. Soc., Perkin Trans. 1* **1993**, 1287−1297.

(10) Schenning, A. P. H. J.; Elissen-Román, C.; Weener, J. W.; Baars, M. W. P. L.; van der Gaast, S. J.; Meijer, E. W. Amphiphilic dendrimers as building blocks in supramolecular assemblies. *J. Am. Chem. Soc.* **1998**, *120*, 8199−8202.

(11) Wang, B. B.; Zhang, X.; Jia, X. R.; Li, Z. C.; Wei, Y. Self-assembly of a new class of amphiphilic poly(amidoamine) dendrimers and their electrochemical properties. *J. Polym. Sci., Part A: Polym. Chem.* **2005**, *43*, 5512−5519.

(12) Wang, B. B.; Zhang, X.; Jia, X. R.; Luo, Y. F.; Sun, Z.; Yang, L.; Ji, Y.; Wei, Y. Poly(amidoamine) dendrimers with phenyl shell: Fluorescence and aggregation behavior. *Polymer* **2004**, *45*, 8395−8402.

(13) Wang, B. B.; Zhang, X.; Jia, X. R.; Li, Z. C.; Ji, Y.; Yang, L.; Wei, Y. Fluorescence and aggregation behavior of poly(amidoamine) dendrimers peripherally modified with aromatic chromophores: The effect of dendritic architectures. *J. Am. Chem. Soc.* **2004**, *126*, 15180−15194.

(14) Gröhn, F.; Klein, K.; Koynov, K. A novel type of vesicles based on ionic and $\pi-\pi$ interactions. *Macromol. Rapid Commun.* **2010**, *31*, 75−80.

(15) Cao, W.; Zhu, L. Synthesis and unimolecular micelles of amphiphilic dendrimer-like star polymer with various functional surface groups. *Macromolecules* **2011**, *44*, 1500−1512.

(16) Boas, U.; Heegaard, P. M. H. Dendrimers in drug research. *Chem. Soc. Rev.* **2004**, *33*, 43−63.

(17) Malhotra, S.; Bauer, H.; Tschiche, A.; Staedtler, A. M.; Mohr, A.; Calderón, M.; Parmar, V.; Hoeke, L.; Sharbati, S.; Einspanier, R.; Haag, R. Glycine-terminated dendritic amphiphiles for nonviral gene delivery. *Biomacromolecules* **2012**, *13*, 3087−3098.

(18) Nawaz, S.; Carbon, P. Stability of amphiphilic dendrimers at the water/air interface. *J. Phys. Chem. B* **2011**, *115*, 12019−12027.

(19) Hung, W. I.; Hung, C. B.; Chang, Y. H.; Dai, J. K.; Li, Y.; He, H.; Chen, S. W.; Huang, T. C.; Wei, Y.; Jia, X. R.; Yeh, J. M. Synthesis and electroactive properties of poly(amidoamine) dendrimers with an aniline pentamer shell. *J. Mater. Chem.* **2011**, *21*, 4581−4587.

(20) Santo, M.; Fox, M. A. Hydrogen bonding interactions between Starburst dendrimers and several molecules of biological interest. *J. Phys. Org. Chem.* **1999**, *12*, 293−307.

(21) Tomalia, D. A.; Baker, H.; Dewald, J.; Hall, M.; Kallos, G.; Martin, S.; Roeck, J.; Ryder, J.; Smith, P. A new class of polymers: Starburst-dendritic macromolecules. *Polym. J.* **1985**, *17*, 117−132.

(22) Huang, L. H.; Hu, J.; Lang, L.; Wang, X.; Zhang, P. B.; Jing, X. B.; Wang, X. H.; Chen, X.; Lelkes, P. I.; MacDiarmid, A. G.; Wei, Y. Synthesis and characterization of electroactive and biodegradable ABA block copolymer of polylactide and aniline pentamer. *Biomaterials* **2007**, *28*, 1741−1751.

(23) Wei, Y.; Yang, C.; G, W.; Feng, G. A new synthesis of aniline oligomers with three to eight amine units. *Synth. Met.* **1997**, *84*, 289−291.

(24) Yan, Q.; Yuan, J. Y.; Kang, Y.; Yin, Y. Dynamic supramacromolecular self-assembly: deformable polymer fabricated nanostructures through a host-controlled approach. *Polym. Chem.* **2010**, *1*, 423−425.

(25) Lee, K.-H.; Song, D. H.; Park, B. J.; Chin, I.-J.; Choi, H. J. Structures of polyaniline bases: Semi-empirical computations. *Macromol. Theory Simul.* **2009**, *18*, 287−298.

(26) Israelachivili, J. N. *Intermolecular and Surface Forces*; Academic Press: New York, 1985.

(27) Tsuda, K.; Dol, G. C.; Gensch, T.; Hofkens, J.; Latterini, L.; Weener, J. W.; Mwijer, E. W.; Schryver, F. C. Fluorescence from azobenzene functionalized poly(propylene imine) dendrimers in self-assembled supramolecular structures. *J. Am. Chem. Soc.* **2000**, *122*, 3445−3452.

(28) Cho, M. S.; Cho, Y. H.; Choi, H. J.; Jhon, M. S. Synthesis and electroheological characteristics of polyaniline-coated poly(methyl methacrylate) microsphere: Size effect. *Langmuir* **2003**, *19*, 5875−5881.

(29) Lee, I. S.; Cho, M. S.; Choi, H. J. Preparation of polyaniline coated poly(methyl methacrylate) microsphere by graft polymerization and its electroheology. *Polymer* **2005**, *46*, 1317.

(30) Fang, F. F.; Liu, Y. D.; Lee, I. S.; Choi, H. J. Well controlled core/shell type polymeric microshperes coated with conducting polyaniline: fabrication and electrorheology. *RSC Adv.* **2011**, *1*, 1026−1032.

(31) Li, J.; Qin, D.; Baker, J. J. R.; Tomalia, D. A. The Characterization of high generation poly(amidoamine) G9 dendrimers by atomic force microscopy (AFM). *Macromol. Symp.* **2001**, *166*, 257−269.

(32) Betley, T. A.; Holl, M. M. B.; Orr, B. G.; Swanson, D. R.; Tomalia, D. A.; Baker, J. J. R. Trapping mode atomic force microscopy investigation of poly(amidoamine) dendrimers: effects of substrate and pH on dendrimer deformation. *Langmuir* **2001**, *17*, 2768−2773.

(33) Miller, L. L.; Hashimoto, T.; Tabakovic, I.; Swanson, D. R.; Tomalia, D. A. Delocalized π-stacks formed on dendrimers. *Chem. Mater.* **1995**, *7*, 9−11.
(34) Liu, Y.; Bryantsev, V. S.; Diallo, M. S.; Goddard, W. A. I. PAMAM dendrimers undergo pH responsive conformational changes without swelling. *J. Am. Chem. Soc.* **2009**, *131*, 2798−2799.
(35) Chao, D.; Lu, X.; Chem, J.; Liu, X.; Zhang, W.; Wei, Y. Synthesis and characterization of electroactive polyamide with amine-capped aniline pentamer and ferrocene in the main chain by oxidative coupling polymerization. *Polymer* **2006**, *47*, 2643−2648.
(36) Pouget, J. P.; Jozefowicz, M. E.; Epstein, A. J.; Tang, X.; MacDiarmid, A. G. X-ray structure of polyaniline. *Macromolecules* **1991**, *24*, 779−789.
(37) Wang, Y.; Grayson, S. M. Approaches for the preparation of non-linear amphiphilic polymers and their applications to drug delivery. *Adv. Drug Delivery Rev.* **2012**, *64*, 852−865.
(38) Sadekar, S.; Ghandehari, H. Transepithelial transport and toxicity of PAMAM dendrimers: Implications for oral drug delivery. *Adv. Drug Delivery Rev.* **2012**, *64*, 571−588.
(39) Svenson, S.; Tomalia, D. A. Dendrimers in biomedical applications—reflections on the field. *Adv. Drug Delivery Rev.* **2005**, *57*, 2106−2129.